

Photolabile linkers: exploiting labile bond chemistry to control mode and rate of hydrogel degradation and protein release

Paige J. LeValley, Raghupathi Neelarapu, Bryan Sutherland, Srimoyee Dasgupta, Christopher J Kloxin, and April M. Kloxin

J. Am. Chem. Soc., **Just Accepted Manuscript** • DOI: 10.1021/jacs.9b11564 • Publication Date (Web): 09 Feb 2020

Downloaded from pubs.acs.org on February 9, 2020

Just Accepted

“Just Accepted” manuscripts have been peer-reviewed and accepted for publication. They are posted online prior to technical editing, formatting for publication and author proofing. The American Chemical Society provides “Just Accepted” as a service to the research community to expedite the dissemination of scientific material as soon as possible after acceptance. “Just Accepted” manuscripts appear in full in PDF format accompanied by an HTML abstract. “Just Accepted” manuscripts have been fully peer reviewed, but should not be considered the official version of record. They are citable by the Digital Object Identifier (DOI®). “Just Accepted” is an optional service offered to authors. Therefore, the “Just Accepted” Web site may not include all articles that will be published in the journal. After a manuscript is technically edited and formatted, it will be removed from the “Just Accepted” Web site and published as an ASAP article. Note that technical editing may introduce minor changes to the manuscript text and/or graphics which could affect content, and all legal disclaimers and ethical guidelines that apply to the journal pertain. ACS cannot be held responsible for errors or consequences arising from the use of information contained in these “Just Accepted” manuscripts.

Photolabile linkers: exploiting labile bond chemistry to control mode and rate of hydrogel degradation and protein release

Paige J. LeValley,^a Raghupathi Neelarapu,^b Bryan P. Sutherland,^a Srimoyee Dasgupta,^c
Christopher J. Kloxin,^{a,c*} April M. Kloxin^{a,c,*}

a. Department of Chemical and Biomolecular Engineering, University of Delaware, Newark, DE 19716, United States

b. Department of Chemistry and Biochemistry, University of Delaware, Newark, DE 19716, United States

c. Department of Material Science and Engineering, University of Delaware, Newark, DE 19716, United States

Abstract

Photolabile moieties have been utilized in applications ranging from peptide synthesis and controlled protein activation to tunable and dynamic materials. The photochromic properties of nitrobenzyl (NB) based linkers are readily tuned to respond to cytocompatible light doses and are widely utilized in cell culture and other microbiological applications. While widely utilized, little is known about how the microenvironment, particularly confined aqueous environments (*e.g.*, hydrogels), affects both the mode and rate of cleavage of NB moieties, leading to unpredictable limitations in control over system properties (*e.g.*, rapid hydrolysis or slow photolysis). To address these challenges, we synthesized and characterized the photolysis and hydrolysis of NB moieties containing different labile bonds (*i.e.*, ester, amide, carbonate, or carbamate) that served as labile crosslinks within step-growth hydrogels. We observed that NB ester bond exhibited significant rates of both photolysis and hydrolysis, whereas, importantly, the NB carbamate bond had superior light responsiveness and resistance to hydrolysis within the hydrogel microenvironment. Exploiting this synergy and orthogonality of photolytic and hydrolytic degradation, we designed concentric cylinder hydrogels loaded with different cargoes (*e.g.*, model protein with different fluorophores) for either combinatorial or sequential release, respectively. Overall, this work provides new facile chemical approaches for tuning the degradability of NB linkers and an innovative strategy for the construction of multimodal degradable hydrogels, which can be utilized

1
2
3 to guide the design of not only tunable materials platforms but also controlled synthetic protocols
4
5 or surface modification strategies.
6
7
8
9
10
11
12
13
14
15
16
17
18
19
20
21
22
23
24
25
26
27
28
29
30
31
32
33
34
35
36
37
38
39
40
41
42
43
44
45
46
47
48
49
50
51
52
53
54
55
56
57
58
59
60

Introduction

Materials with light responsive properties, especially hydrogels, are useful for a multitude of applications including self-healing,¹ biosensing,² drug delivery,³ polymer structure,⁴ and tissue engineering⁵. Photolabile materials are widely used because they offer on-demand spatial and temporal control over system properties for designing tunable platforms, building upon seminal works that have utilized photolabile groups as cages to control the activity of small molecules or proteins.⁶⁻⁸ Photolabile chemistries are commonly integrated into the material design as linkers or pendant groups for modulating structure,^{9,10} surface modifications,^{11,12} mechanical properties^{13,14} matrix degradation,^{15,16} or biomolecule presentation,^{17,18} providing opportunities for probing how the timing and magnitude of changes in these properties influence downstream responses. Nitrobenzyl (NB) based linkers are one of the most commonly used classes of photodegradable linkers within this field. The popularity of NB linkers can be attributed, in part, to their responsiveness to cytocompatible doses of light and the observed *in vitro* and *in vivo* biocompatibility of their cleavage products when attached to polymers, which are essential properties in designing materials for biological applications.^{19,20} However, in these applications, variations in the cleavage behavior of NB linkers have emerged that appear to be microenvironment specific, motivating the need for new fundamental studies that inform and enable innovative material designs.

Initial seminal studies incorporating NB linkers within such materials, particularly hydrogels, focused on tuning the absorbance of NB moieties and the rate of photocleavage through modifications to the NB ring, which alter the molar absorptivity, quantum yield, and ultimately half-life of the moiety upon irradiation.^{21,22} In general, substitution of a methyl group in the benzylic position leads to enhancements in photocleavage kinetics along with the added benefit of producing less reactive byproducts compared with the NB without a benzylic substitution.²³ Other modifications that have been investigated include the addition of methoxy

1
2
3 groups to the ring structure of the NB, which broadly increases absorbance of long wavelengths
4 of light but also results in lower quantum yields in comparison to their unmodified counterparts.^{22,24}
5
6 Further, methods for installing orthogonal reactive handles have been investigated to provide
7 mechanisms for installation of NB groups onto polymer backbones or surfaces in addition to
8 conjugation to other molecules.^{19,25} Utilizing these strategies, combinations of different NB
9 moieties have been integrated within the crosslinks to bias the degradation of hydrogels²¹ and
10 within pendant groups to control the release of small molecules²² or peptides.²⁶ Alternatively, such
11 NB groups have been combined to act as a photocage and photocleavable linker, respectively,
12 to control peptide presentation within hydrogels.²⁶ While methods for controlling the
13 photodegradation properties of NB-based materials through ring substitutions are now well
14 established, less is known about how the degradation properties of these materials are impacted
15 by the chemical nature of the photocleavable bond itself.

16
17
18
19
20
21
22
23
24
25
26
27
28
29
30 NB linkers with ester (NB-ester) or amide (NB-amide) photocleavable bonds are widely
31 used for the design of responsive materials and have been observed to have variable degradation
32 properties in different microenvironments. Indeed, while helpful in guiding the initial design for
33 photodegradable applications, many solution-based studies (*i.e.*, small molecule studies in
34 organic solvents owing to solubility) do not accurately represent the hydrogel microenvironment
35 and, consequently, can lack predictivity. For example, solution based studies comparing the
36 photodegradation rate of an NB-ester to NB-amide with the same ring substituents found that the
37 NB-amide degraded at a faster rate than the NB-ester; however, the photodegradation rate of
38 NBs immobilized onto a solid-phase resin was observed to decrease for NB-amides but not with
39 NB-esters.^{23,27} Within the biomaterials community, similar trends have been observed when these
40 linkers were incorporated as crosslinks within hydrogel networks, where switching from the NB-
41 ester to the NB-amide moiety within the crosslinks of poly(ethylene glycol) (PEG) hydrogels has
42 been observed to decrease the rate of photodegradation 3- to 10-fold.²⁸⁻³¹ Interestingly, significant

1
2
3 decreases in rate were not reported for NB-amide moieties used to tether hydrophobic small
4 molecules to the hydrogel network; this potentially points to the importance of the nature of the
5 group proximate to the cleavable bond (*e.g.*, hydrophobic vs. hydrophilic).^{21,22}
6
7

8
9
10 In addition to these complexities associated with photodegradation of NB groups in
11 different microenvironments, the labile bond also has been observed to impact their hydrolytic
12 stability in some applications, which can significantly impact the use of these molecules in
13 systems requiring long term stability in aqueous microenvironments. While hydrolysis of NB
14 linkers often is not characterized, NB-esters incorporated within step-growth PEG-based
15 hydrogels have been observed to exhibit appreciable hydrolysis under physiological pH even over
16 short times (hours to days), limiting user control over the properties of these systems at longer
17 time scales (*e.g.*, *in situ* tuning of structure, modulus, release over many days to weeks).^{30,32}
18
19 Cumulatively, these examples show the importance of the microenvironment in the
20 photodegradation behaviors of NB moieties and the potential tunability associated with these
21 groups for modulating properties within different chemical, material, and biological contexts.
22
23
24
25
26
27
28
29
30
31
32
33

34 Broadly accessible strategies for addressing these disparities in degradation behaviors
35 within hydrogels are needed for both fundamental insights and improved tools for materials
36 design. To address this, in this work, we present a simple and innovative approach for tuning the
37 rates of hydrolysis and photolysis of NB-linked step-growth hydrogels through modifications to
38 labile bond chemistry. Specifically, we establish alternatives to the NB-ester and NB-amide linking
39 moieties to address the limitations presented by these two linkers while enhancing the toolbox of
40 light responsive chemistries that can be employed within such polymeric materials. Four different
41 NB labile bond chemistries (NB-ester, NB-amide, NB-carbonate, and NB-carbamate) were
42 synthesized and characterized as crosslinks within well-defined hydrogel networks formed with
43 strain-promoted azide-alkyne cycloaddition (SPAAC) crosslinking chemistry (**Figure 1A-B**). We
44 hypothesized that the NB-carbonate and NB-carbamate linkers would impart increased stability
45
46
47
48
49
50
51
52
53
54
55
56
57
58
59
60

in water while maintaining the rate of photolysis, based on the known mechanisms of cleavage for these alcohol-based nitrobenzyl groups.^{33,34} Both, the photolytic and hydrolytic behavior of the four different NB linkers was investigated, establishing key differences in susceptibility to stimuli and the timescales of these different degradation mechanisms (**Figure 1C-D**). To employ the resulting orthogonal versus dual modes of degradation, sequential or combinatorial release of encapsulated model cargoes (*e.g.*, a protein labeled with complementary fluorophores) was demonstrated with concentric cylinder hydrogels integrating different labile linkers for quantitative comparison with reaction kinetics. These studies provide new and accessible chemical approaches for independent control of photolysis and hydrolysis and unique insights into the effect of NB labile bond chemistry on material degradation for guiding the design of photolabile systems for a range of applications, from soft materials and nanoparticles to peptides and proteins.

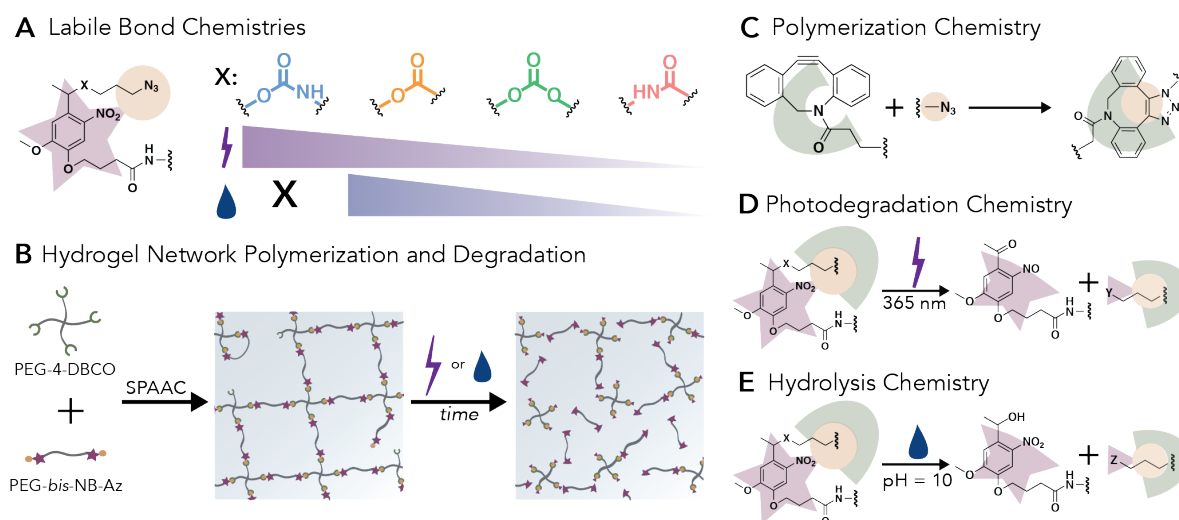


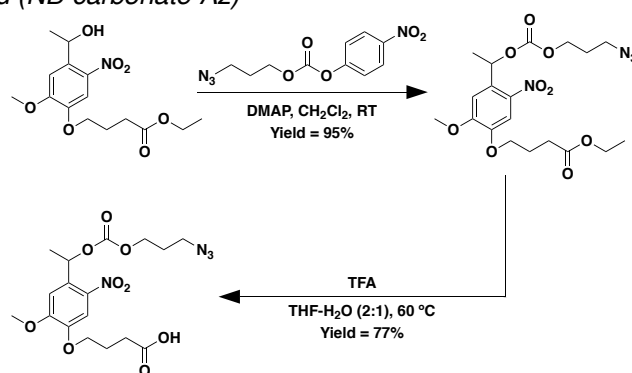
Figure 1. Overview of approach. (A) Nitrobenzyl (NB) moieties were synthesized to have various labile bond chemistries, X: carbamate (blue), ester (orange), carbonate (green), or amide (pink). (B) Hydrogel networks formed with NB containing crosslinks were degraded over short time scales by light irradiation or over long time scales by incubation in aqueous conditions. (C) Hydrogels were polymerized using a SPAAC between PEG-4-DBCO and photodegradable PEG-*bis*-NB-azide (Az) to form triazole linkages. (D) Upon irradiation with 365 nm light the incorporated NB moiety undergoes an irreversible photocleavage event that breaks hydrogel crosslinks, leading to hydrogel erosion. The cleavable bond, X, dictates the rate of photodegradation and the functionality of the cleavage products formed, Y. (E) Additionally, the nature of the cleavable bond influences the ability of the hydrogel to degrade in aqueous environments; here, a hydroxyl is shown, which would be generated upon hydrolysis of NB-ester, NB-carbonate, and NB-carbamate linkers, whereas an amine would be generated upon hydrolysis of NB-amide linkers. The functionality of the hydrolysis cleavage product is represented by, Z.

Results and Discussion

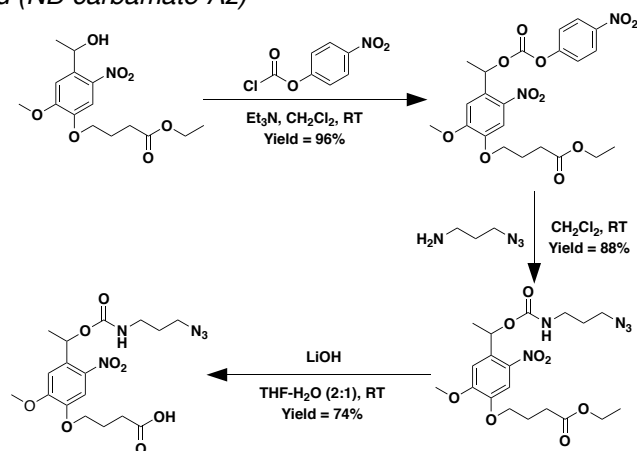
Synthesis of PEG-NB crosslinkers

In addition to synthesizing a NB-ester-azide (see SI, Figure S4), we designed and successfully synthesized two new NB linkers: a NB-carbonate or NB-carbamate labile linker possessing azide functionality. For the synthesis of the NB-carbonate-azide, 3-azidopropyl (4-nitrophenyl) carbonate was reacted with ethyl 4-(4-(1-hydroxyethyl)-2-methoxy-5-nitrophenoxy) butanoate to form the ester protected product, which was subsequently deprotected to yield the desired azide functionalized carbonate-linked NB moiety (Scheme 1, SI, and Figure S9). A slightly modified procedure was utilized to synthesize the NB-carbamate-azide, owing to safety concerns with forming the 3-azidopropyl (4-nitrophenyl) carbamate. 4-nitrophenyl chloroformate was first reacted with ethyl 4-(4-(1-hydroxyethyl)-2-methoxy-5-nitrophenoxy) butanoate followed by the addition of 3-azidopropan-1-amine to yield the ester protected carbamate-linked product, which was subsequently cleaved to yield the desired azide-functionalized carbamate-linked NB moiety (Scheme 2, SI, and Figure S12).

Scheme 1. Synthesis of 4-(4-(1-(((3-azidopropoxy)carbonyl)oxy)ethyl)-2-methoxy-5-nitrophenoxy)butanoic acid (NB-carbonate-Az)



Scheme 2. Synthesis of 4-(4-(1-(((3-azidopropoxy)carbamoyl)oxy)ethyl)-2-methoxy-5-nitrophenoxy)butanoic acid (NB-carbamate-Az)



These linkers, along with a NB-ester and NB-amide, were attached to linear PEG diamine monomers via amide coupling (see SI) to form diazide end-functionalized linear photodegradable PEG (PEG-*bis*-NB-azide) (Figure S14 – S17) to be used as crosslinks in hydrogel networks. The successful synthesis of NB moieties with carbonate and carbamate labile bonds represents two new linker chemistries that, to our knowledge, have yet to be characterized as crosslinks within hydrogel matrices. While utilized here for hydrogel formation, the design of these photolabile moieties with an azide and a carboxylic acid handle provides opportunities for facile conjugations to other amine or hydroxyl presenting molecules, including proteins and peptides.

Photolytic behavior of NB containing hydrogels

The linear viscoelastic properties of the hydrogels can be utilized to monitor both the polymerization and degradation behaviors of these networks, where the storage modulus correlates directly with bond formation and cleavage, respectively. Well-defined step-growth hydrogels were formed using a SPAAC reaction between cyclooctyne end-functionalized four-arm PEG (PEG-4-DBCO, Figure S18) and PEG-*bis*-NB-azide (**Figure 1B**). SPAAC is a biologically orthogonal reaction chemistry that is widely used for both materials synthesis and

1
2
3 bioconjugation reactions. The polymerization time and storage modulus of the four different
4 hydrogel formulations (*i.e.*, containing either an ester, an amide, a carbonate, or a carbamate
5 labile bond) were determined using dynamic time sweep measurements conducted *in situ* on a
6 rheometer within the linear viscoelastic regime for these materials. PEG-4-DBCO and PEG-*bis*-
7 NB-azide precursor solutions at a 1:1 stoichiometric ratio of cyclooctyne to azide and final polymer
8 concentration of approximately 5 wt% were mixed to form hydrogels. To ensure that degradation
9 results were not convoluted by different starting moduli, the four hydrogel formulations
10 investigated were slightly adjusted such that the final storage moduli of all samples were
11 statistically the same prior to degradation (Figure S26).
12
13
14
15
16
17
18
19
20
21
22

23 The effect of NB labile bond chemistry on the rate of photodegradation was investigated by
24 monitoring the storage modulus of hydrogels during irradiation with 365 nm light at an intensity of
25 4 mW cm⁻² (Figure S25). Within the time scales of interest, we assumed that bond cleavage was
26 strictly due to irradiation, eventually leading to complete hydrogel degradation (*i.e.*, when the
27 hydrogel can no longer store stress).^{35,36} Based on rubber elasticity theory and hydrogel network
28 connectivity, the storage modulus of the hydrogel is directly related to the crosslink density of the
29 network and therefore bond cleavage, which can be modeled using first-order reaction kinetics
30 (*i.e.*, storage modulus (G') \propto crosslink density (ρ_x) $\propto e^{-k_{eff}t}$).^{30,37} This relationship between the
31 effective first order rate constant and the storage modulus of the network affords the opportunity
32 to fit linearized rheological data to determine the effective first order rate constant for the hydrogel.
33
34 Specifically, the natural log of the normalized modulus was plotted versus time and fit using linear
35 regression over the first two minutes of light irradiation to determine the effective first order
36 photodegradation constant for each linker within the hydrogel (Figure S27). To obtain the
37 photodegradation rate, k , for the NB moiety within the hydrogels, the effective first order rate
38 constant was divided by two as a decrease in crosslinking density occurs due to a photolytic
39
40
41
42
43
44
45
46
47
48
49
50
51
52
53
54
55
56
57
58
59
60

cleavage event on either side of the elastically active chain between nodes within the crosslinked network (*e.g.*, PEG-*bis*-NB).³⁸ Importantly, using this approach we found that the fastest rate of photodegradation occurred in hydrogels formed with the NB-carbamate linker followed by the NB-ester, the NB-carbonate, and finally the NB-amide linkers (**Figure 2B**).

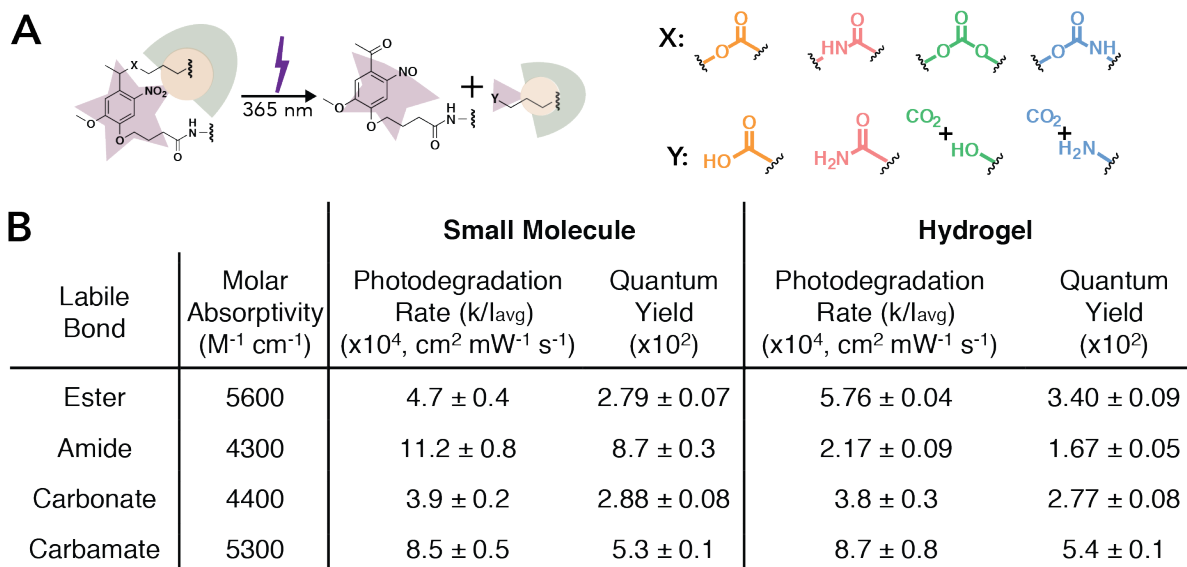


Figure 2. Rate of small molecule and hydrogel degradation in response to light. (A) The NB moiety incorporated within the hydrogel backbone undergoes a β -elimination reaction upon 365 nm light irradiation. Four different photocleavable bonds, X, were investigated, all of which lead to different cleavage products, Y (as confirmed by NMR and mass spectrometry, Figure S21 – S24 and Table S1 – S4). (B) Small molecule NBs ($I_0 = 10 \text{ mW cm}^{-2}$ resulting in an $I_{\text{avg}} = 7.8 \text{ mW cm}^{-2}$) and photolabile hydrogels ($I_0 = 4 \text{ mW cm}^{-2}$ resulting in an $I_{\text{avg}} = 3.9 \text{ mW cm}^{-2}$) were irradiated with 365 nm light to determine the first order photodegradation rate and quantum yield. The molar absorptivity was determined using the absorbance of each small molecule NB moiety at 365 nm. First order rate constants were determined for each of the four NB groups with different cleavable bonds in solution and within hydrogels (Figure S20 and S27) and used to calculate the quantum yield. All formulations (NB-ester vs. NB-Amide vs. NB-carbonate vs. NB-carbamate) were found to be statistically different except that determined for the ester and carbonate in solution and for the amide and carbonate in hydrogels ($p = 0.05$). For full statistical analysis see Tables S5, S7, and S8. The data shown illustrate the mean ($n = 3$) with error representing standard error.

The determined rate constants for the cleavage of the NB-ester and NB-amide moieties integrated within the crosslinks of hydrogels follow trends observed in literature, with the NB-amide bond degrading slower than the NB-ester bond within the same hydrogel microenvironment. Specifically, from previous work published by our group, the photodegradation of NB-amide bonds contained within hydrogel crosslinks were determined to have a

1
2
3 photodegradation rate that was ~2.8x slower than an identically formed hydrogel containing NB-
4 ester crosslinks, consistent with the results found here.^{30,31} To compare the photodegradation
5 properties between NBs in solution and those integrated within the crosslinks of hydrogels, the
6 photodegradation kinetics of the small molecule NB groups were assessed through solution-
7 based NMR studies performed in deuterated water containing 5% DMSO and 1x PBS salts, both
8 used to improve solubility of NB moieties where the latter mimics hydrogel conditions. As the
9 PEG-NB-amide-azide was synthesized using a NB-amide-Fmoc, followed by deprotection and
10 amide coupling of 4-azidobutanoic acid, a NB-amide-acetyl was synthesized as an analog, which
11 has been used as a model NB-amide in previous studies and is more representative of the NB-
12 amide within the crosslink than the Fmoc derivative.²³ Similar to previous reports, we observed
13 that the rate of the NB-amide was fastest in solution followed by the NB-carbamate, NB-ester,
14 and NB-carbonate (**Figure 2B**, Figure S20).²³ Interestingly, while the NB-ester, NB-carbonate,
15 and NB-carbamate linkers exhibited no significant differences in photodegradation rate between
16 the solution and hydrogels, the NB-amide linker had a significantly reduced photodegradation rate
17 upon incorporation into hydrogels (>5x, **Figure 2B**). Of note is the NB-carbamate, which exhibited
18 a photodegradation rate that was significantly faster than all 3 of the other photolabile bonds within
19 the hydrogel environment, demonstrating the utility in exploiting NB labile bond chemistry for
20 tuning degradation properties.

21
22
23 Beyond providing a new reactive handle for rapid photocleavage, the observation of rapid
24 degradation of the NB-carbamate linker relative to the NB-amide linker within hydrogels provides
25 some new insight into the origin of disparities for photocleavage of the NB-amide in solution
26 versus in hydrogel microenvironments. As noted earlier, when the NB-amide has been utilized as
27 a linker in a confined environment, such as through attachment to resin in peptide synthesis²³ or
28 utilization as a crosslink within a hydrogel,³¹ the rate of photodegradation is significantly slowed.
29 This observed decrease in photodegradation rate has been hypothesized by others as an artifact

1
2
3 of light scattering, shadowing effects, and/or swelling/solvation properties of the support.²³ As
4 demonstrated by our data above and consistent with previous reports on resin,²³ the NB-amide
5 exhibited slowed photodegradation when crosslinked within hydrogels in comparison with solution
6 based photodegradation. Of note, amide bond stability has been directly linked to bond rotation
7 and distortion,³⁹ where confinement within a crosslink of a hydrogel network may limit activation
8 of the amide linkage. Additionally, while the incorporation of the NB-amide within hydrogel
9 crosslinks leads to slowed photodegradation, using it to tether hydrophobic molecules to a
10 hydrogel network has been observed to not drastically decrease the photodegradation rate
11 compared to what has been previously reported in solution.^{22,23} In mechanistic studies, it has been
12 reported that destabilization of the reaction intermediates that the NB moiety goes through upon
13 the light initiated photoisomerization (Norrish type II) reaction leads to slowed photodegradation
14 and is related to the labile bond.³³ In this broader context, we speculate that a combination of the
15 microenvironment effects contribute to the observed disparity in the rate of NB-amide degradation
16 in the hydrogel vs. in free solution: confinement exerted on the amide bond upon being integrated
17 into the hydrogel network leads to changes in bond conformation and hydration that may increase
18 the thermodynamic driving force required for the photoisomerization reaction. Regardless of
19 mechanism, our data demonstrate quantitatively what has been observed anecdotally to date: a
20 significantly slowed rate of NB-amide photodegradation upon incorporation within the crosslinks
21 of hydrogels, which remains a consistent a challenge for their use in specific applications.
22
23
24
25
26
27
28
29
30
31
32
33
34
35
36
37
38
39
40
41
42
43
44

45 One additional observation is that the NB-amide hydrogels did not undergo complete hydrogel
46 erosion within 30 min of continuous irradiation, whereas all hydrogels with the other NB labile
47 bonds did completely degrade. Specifically, the NB-amide hydrogel storage modulus never
48 crossed over the loss modulus upon light irradiation (Figure S25), and a hydrogel layer was still
49 observed upon lifting the rheometer plate. We postulated that this incomplete degradation was
50 caused by a shift in the rate-limiting reaction intermediate due to the participation of the amide in
51
52
53
54
55
56
57
58
59
60

1
2
3 the Norris type-II reaction.^{33,40} To test this and examine a potential means for rescuing the
4 photodegradability of the NB-amide, we utilized a carbonyl scavenger (semicarbazide), which has
5 been reported in the literature as an effective method to overcome such decreases in
6 photodegradation rate.^{7,23} Notably, with this approach, we observed full degradation of the amide-
7 linked hydrogel in the presence of the carbonyl scavenger, with complete degradation within a
8 timeframe commensurate with the photodegradation rate observed at early irradiation time
9 (Figure S28). This ability of an immobilized NB-amide to fully degrade in the presence of a
10 carbonyl scavenger has been observed in literature and was hypothesized by others to be caused
11 by the scavenger aiding in the photocleavage mechanism.²³ More broadly, our new study here
12 demonstrates a method for achieving complete photodegradation of NB-amide crosslinked
13 hydrogels through the utilization of a carbonyl scavenger. As a whole, our investigations of the
14 rates of photolysis demonstrate how different NB labile bond chemistries can be used to tune the
15 effective rates of photodegradation.
16
17
18
19
20
21
22
23
24
25
26
27
28
29
30
31
32
33

34 *Hydrolytic behavior of NB containing hydrogels*

35
36 Hydrolysis of the NB labile bond is another method by which these hydrogels can degrade in
37 response to a stimulus over longer times (*e.g.*, days to months). Understanding the rate of
38 hydrolysis of NB containing hydrogels is critical for establishing relevant timescales for tuning of
39 network properties either solely by photolysis, hydrolysis, or dually with both, as desired for the
40 application of interest. To investigate any differences in hydrogel responses to aqueous
41 environments, we conducted an accelerated hydrolysis test: hydrogels were incubated in PBS pH
42 = 10, and the hydrogel volume was measured over 72 h (**Figure 3**).^{41–43} Previous reports have
43 demonstrated the relevance of accelerated hydrolysis tests for predicting trends in hydrolysis
44 under physiological conditions, supporting the relevance of this approach in assessing the long
45 term stability of hydrolytically sensitive hydrogels.⁴³ Under these conditions, hydrogels undergo
46
47
48
49
50
51
52
53
54
55
56
57
58
59
60

bulk degradation that leads to an increase in hydrogel volume ($\rho_x \propto Q = V/V_0$) until a single chain no longer spans the percolated network and the hydrogel is fully degraded (e.g., hydrogel undergoes reverse gelation). For NB-ester hydrogels, a rapid swelling followed by complete degradation was observed within 1 h in the incubation buffer, as expected based upon the known susceptibility of ester bonds to hydrolysis (**Figure 3**). NB-ester hydrogels exhibited the fastest degradation rate, followed by that of the NB-carbonate and NB-amide. Pivotaly, no significant degradation of the NB-carbamate hydrogels was observed under these conditions, with only minimal volume changes after an initial equilibrium swelling, similar to the behavior observed in the non-degradable control hydrogels.

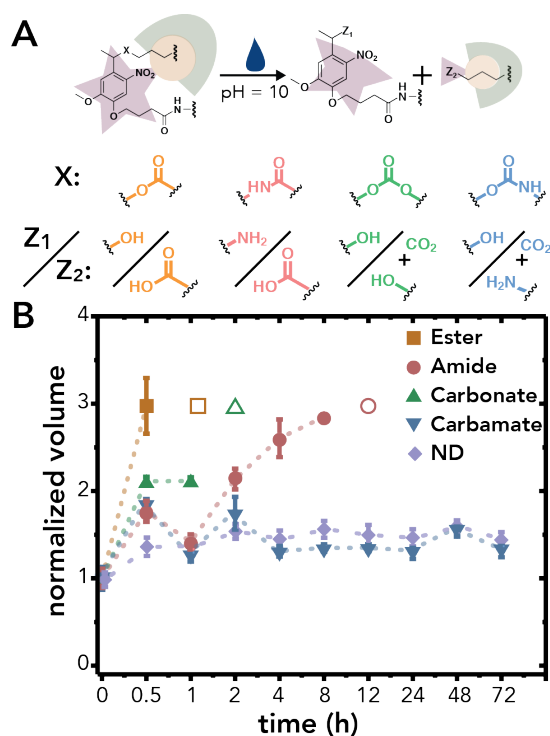


Figure 3. Hydrolysis of NB-linked hydrogels. (A) The cleavable bond (X) of the NB group dictates the rate of hydrogel hydrolysis and the products formed, where Z₁ and Z₂ represent the products formed on the NB ring and cleaved chain, respectively. (B) Hydrogel volume was monitored over 72 h as a semi-quantitative measure of the rate of hydrolysis, where hydrogels were incubated in PBS pH = 10 for accelerated hydrolysis. Hydrogels crosslinked with ether-linked PEG-*bis*-azide served as a non-degradable (ND) control. The empty shapes indicate complete hydrogel degradation which occurred at < 1 h for NB-ester, < 2 h for NB-carbonate, and < 12 h for NB-amide. The volume was normalized to the equilibrium swollen hydrogel volume at t = 0 h. The data shown illustrate the mean (n = 3) with error bars representing standard error.

1
2
3 The hydrolysis chemistry of ester, amide, carbonate, and carbamate labile bonds has been
4 well established in literature;^{44–46} as expected, the ester labile bond exhibited both rapid
5 photodegradation and hydrolysis, whereas the amide labile bond showed a slower
6 photodegradation rate and increased hydrolytic stability, comparatively.^{30,31} Excitingly, the
7 carbonate and carbamate labile bonds offer degradation properties that differ from the NB labile
8 bond chemistries commonly used within hydrogels. The carbamate labile bond is especially
9 appealing with both a rapid photodegradation rate and prolonged hydrolytic stability. To confirm
10 that the trends observed using the accelerated hydrolysis test would hold under physiological
11 conditions, hydrogels were incubated in PBS (pH = 7.4, containing 1% penicillin/streptomycin
12 and 0.2% fungizone) at 37 °C with 5% CO₂, and the volume was monitored for more than one
13 month (Figure S30). Indeed, the trends observed from the accelerated hydrolysis test held, with
14 the NB-ester degrading within 21 days, the NB-carbonate hydrogels degrading within 49 days,
15 and the NB-amide, NB-carbamate, and non-degradable formulations following trends observed
16 in the accelerated hydrolysis test. These data further support the use of accelerated hydrolysis
17 conditions to quickly assess the long term aqueous stability of these NB hydrogel formulations.
18 Understanding the interplay between labile bond chemistry and degradation properties is
19 important when designing photodegradable hydrogel-based platforms for various applications,
20 where both the photolytic and hydrolytic properties of the different NB-linkers can be utilized to
21 engineer systems that degrade over multiple time scales based upon the stimulus applied.
22
23
24
25
26
27
28
29
30
31
32
33
34
35
36
37
38
39
40
41
42
43
44
45
46

47 *Dual and sequential protein release from concentric cylinder hydrogel utilizing different NB linkers*

48
49 Materials that respond to multiple stimuli across various time scales are of interest for a wide
50 range of applications from controlled surface modifications to tunable cell scaffolds. One
51 application of broad interest is the design of materials that can deliver multiple therapies in either
52 a combined or sequential manner. For example, different temporal combinations of nivolumab
53
54
55
56
57
58
59
60

1
2
3 (anti-CTLA4) and ipilimumab (anti-PD1) have proven beneficial for the treatment of advanced
4 melanoma.⁴⁷ As a proof-of-concept toward such combination therapies, dually functional
5 concentric cylinder hydrogels were formed to take advantage of the different NB linker hydrolytic
6 and photolytic properties for creating either a combined or sequential release profile. Specifically,
7 NB-ester and NB-carbamate hydrogel precursor solutions were loaded with a model protein
8 labeled with different fluorophores (BSA-Alexa Fluor (AF) 488 and BSA-AF647, respectively), and
9 hydrogels were formed sequentially as concentric cylinders using custom designed molds (Figure
10 S31). These two formulations were chosen because they have similar photolytic behavior, but
11 opposite hydrolytic behavior, providing a mechanism for creating combined or sequential release
12 profiles. Here, BSA labeled with complementary fluorophores was selected as model cargoes for
13 quantitative comparison of release profiles to each other and to hydrogel degradation kinetics,
14 where encapsulated BSA is known to serve as an effective surrogate for and model of bioactive
15 therapeutic proteins.⁴⁸

16
17
18
19
20
21
22
23
24
25
26
27
28
29
30
31
32 First, the similar photodegradation rates of the NB-ester and NB-carbamate linkers were
33 utilized to create a combined release profile of BSA-AF488 and BSA-AF647 upon 365 nm light
34 irradiation ($I_0 = 10 \text{ mW cm}^{-2}$), monitored using confocal microscopy. The fluorescent intensity
35 within each of the hydrogel regions was monitored over time and found to decrease at similar
36 rates within both hydrogel layers (**Figure 4A**). As these are optically thick constructs, the
37 hydrogels degrade by surface erosion, which is observed when looking at the z-projections of the
38 hydrogel over time where the relative height of each layer was observed to decrease after each
39 irradiation period (**Figure 4B**).

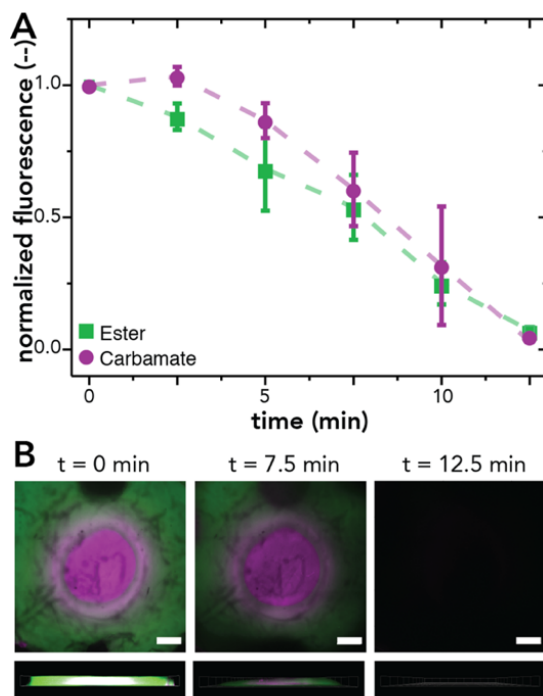


Figure 4. *Combinatorial protein release from dually functional concentric cylinder hydrogels.* NB-ester (BSA-AF488 labeled) and NB-carbamate (BSA-AF647 labeled) dually functional concentric cylinder hydrogels were formed and subsequently irradiated with light (365 nm, $I_0 = 10 \text{ mW cm}^{-2}$) to demonstrate quantitatively the combined release of multiple components dictated by photodegradation kinetics of the respective linkers. (A) The normalized intensity of each region of the concentric cylinder hydrogels was monitored over time and observed to decrease at a similar rate for both layers. (B) Representative images of the surface (top) and side (bottom, $200 \mu\text{m}$ z-stack) of concentric cylinder hydrogels at 0 min (left), 7.5 min (middle), and 12.5 min (right). The data shown illustrate the mean ($n = 3$) with error bars representing standard error. No statistical differences observed between compositions at each time point ($p = 0.05$). Scale bars $500 \mu\text{m}$.

Next, the sequential release of these model cargoes from the concentric cylinder hydrogels was investigated by deploying the opposite hydrolysis behavior exhibited by the NB-ester and the NB-carbamate linkers. The hydrogels were first incubated in PBS pH = 10 for 60 min, degrading the NB-ester layer and releasing BSA-AF488. The remaining hydrogel was subsequently irradiated with 365 nm light ($I_0 = 10 \text{ mWcm}^{-2}$) to degrade the NB-carbamate layer and release BSA-AF647, and the fluorescent intensity within each layer was monitored over the time course of the experiment as before. Importantly, the fluorescent intensity of the NB-ester layer decreased over the 60 min of incubation within basic buffer conditions, releasing the BSA-AF488, followed

1
2
3 by rapid release of the BSA-AF647 from the degrading NB-carbamate layer upon irradiation with
4 light (**Figure 5**). Note, on average, a small segment of hydrogel at the edge of the NB-ester layer
5 remained at 60 min for the hydrogel samples tested, leading to the average normalized
6 fluorescent intensity above zero prior to the light irradiation; this arises from edge effects where
7 the two formulations (NB-ester and NB-carbamate) mixed causing a zone with different
8 degradation properties.⁴⁹

9
10
11
12
13
14
15
16 These proof-of-concept experiments demonstrated the utility of understanding the modes and
17 rates of degradation of different NB linkers within hydrogels and their applicability for controlling
18 the release of encapsulated cargoes. Previous studies have utilized individual NB moieties, with
19 alterations in the number and nature of substitutions to the NB ring or NB moieties, or an NB
20 moiety in combination with other photolabile groups (*i.e.*, coumarins) to control the release of
21 tethered small molecules^{22,34} and bioactive proteins^{18,25,50} or encapsulated cells.^{21,22,51} Here, we
22 demonstrated a facile method for biasing release of encapsulated cargoes through simple
23 processes. Selection of the labile bond afforded on (pre-programmed) / off control via hydrolysis
24 and externally tunable control via photolysis and can be readily translated for use with other NB
25 ring structures and cargoes (*e.g.*, encapsulated nanoparticles or cells). Through full
26 characterization of both photodegradation and hydrolysis of the NB-linkers, design of material
27 systems with tailorable properties can be achieved for investigating various phenomena in both
28 chemical and biological arenas, whether it be surface modification of nanoparticles or tunable
29 hydrogel scaffolds. For example, in drug delivery applications, like that used to guide our proof-
30 of-concept experiment and of large interest within the biomaterials and polymer communities,
31 layered hydrogels with different NB linkers could be utilized to release multiple therapeutic
32 proteins on different time scales. In particular, the unique materials and designs presented here
33 provide a mechanism to bias the release of encapsulated unmodified proteins using both
34 endogenous and exogenous stimuli, with great potential for enabling combination therapies with
35
36
37
38
39
40
41
42
43
44
45
46
47
48
49
50
51
52
53
54
55
56
57
58
59
60

1
2
3 increased efficacy toward addressing the systemic toxicity that has limited clinical translation of
4 these therapeutic regimes. Additionally, these materials could be designed for 3D hydrogel cell
5 culture applications to study the transition from a healthy to diseased state or influence of matrix
6 properties on cell phenotype and behavior, harnessing the different timescales of degradation
7 that can be achieved with individual or combinations of the NB linkers.⁵ The dual modes of
8 degradation and tailorable degradation rates afforded by these NB groups with different labile
9 bonds also could be integrated into workflows, within polymers, or on substrates for tunable
10 synthetic strategies, structure-properties, or surface chemistries. More broadly, the findings of
11 this work demonstrate that different NB labile bonds exhibit different degrees of hydrolytic stability
12 and has significant implications for the testing and use of NB groups in any aqueous
13 microenvironment, where interest in their translation into the human body continues to grow.⁵²

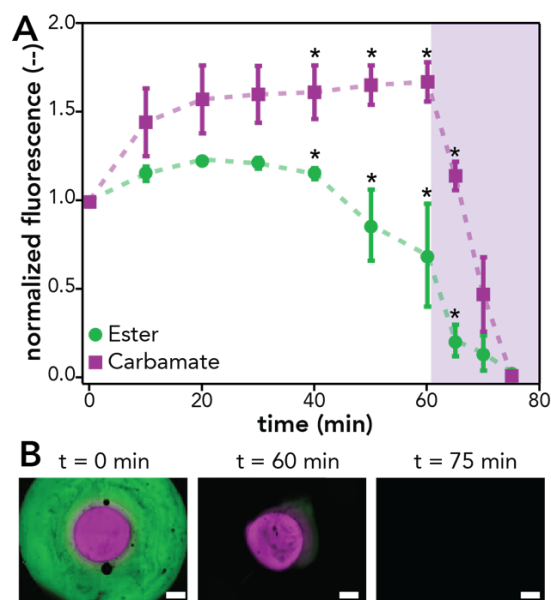


Figure 5. Sequential protein release from dually functional concentric cylinder hydrogels. NB-ester (BSA-AF488 labeled) and NB-carbamate (BSA-AF647 labeled) concentric cylinder hydrogels were formed and subsequently incubated under accelerated hydrolysis conditions (PBS pH = 10) for 60 min followed by irradiation with light (365 nm, $I_0 = 10 \text{ mW cm}^{-2}$). (A) The ester hydrogel layer (green) was observed to degrade during incubation in basic conditions, whereas the carbamate layer (purple) was not observed to degrade until light irradiation. (B) Representative images of the hydrogel at 0 min (left), 60 min (middle), and 75 min (right). The data shown illustrate the mean ($n = 3$) with error bars representing standard error ($p = 0.05$). Scale bars $500 \mu\text{m}$.

Conclusion

In summary, new NB linkers containing a carbonate or carbamate labile bond were synthesized and incorporated into step-growth hydrogels, and their degradation properties compared to established NB linkers with an ester or amide labile bond, addressing limitations of these existing systems in terms of relative rates of hydrolysis and photolysis, respectively. The photodegradation rate of NB-amide moieties in solution versus within hydrogels was found to differ, highlighting the importance of characterizing degradation properties within the microenvironment the moieties will be utilized. Critically, we observed that the NB-carbamate exhibited fast photodegradation kinetics within the hydrogel microenvironment and hydrolytic stability while the NB-ester hydrolytically degraded over the experimental time frame of an accelerated hydrolysis test and hydrolysis test conducted in physiological conditions. Concentric cylinder hydrogels with NB-ester and NB-carbamate linker layers were fabricated to exploit the synergistic degradation modes and rates of these two linkers, allowing quantitative simultaneous release of proteins with either irradiation or sequential hydrolysis and irradiation. This molecular approach to the design of new NB linkers in conjunction with an in-depth understanding of their photolysis and hydrolysis behaviors within aqueous hydrogel environments provides numerous opportunities for the design of innovative degradable materials systems with tunable and controlled properties engineered for applications ranging from surface modifications to tissue engineering.

Associated Content

Supporting information contains experimental and synthetic procedures and additional characterization data (NMR, rheology, and statistical analysis).

Author Information

Corresponding Authors: *cjk@udel.edu and *akloxin@udel.edu

Acknowledgments

The authors would like to thank Dr. Kristi Kiick and Dr. John Koh for helpful conversations regarding hydrogel design and photolabile chemistry. We would like to additionally thank Dr. Megan Smithmyer and Mr. Joseph Spohn for help in the design of the concentric circle hydrogel molds, formed with a 3D printer generously donated by AutoDesk. The research presented here was supported by the Delaware COBRE programs with grants from the NIGMS (P20GM104316 and P30GM110758-02 for core instrument support) and the Delaware Bioscience Center for Advanced Technology (CAT) grant (12A00448), and the W.M. Keck Foundation. We would additionally like to thank support provided through the University of Delaware NMR and Mass Spectrometry Laboratories.

References

- (1) Habault, D.; Zhang, H.; Zhao, Y. Light-Triggered Self-Healing and Shape-Memory Polymers. *Chem. Soc. Rev.* **2013**, *42* (17), 7244–7256.
- (2) Wei, M.; Gao, Y.; Li, X.; Serpe, M. J. Stimuli-Responsive Polymers and Their Applications. *Polym. Chem.* **2017**, *8* (1), 127–143.
- (3) Alvarez-Lorenzo, C.; Bromberg, L.; Concheiro, A. Light-Sensitive Intelligent Drug Delivery Systems. *Photochem. Photobiol.* **2009**, *85* (4), 848–860.
- (4) Chatani, S.; Kloxin, C. J.; Bowman, C. N. The Power of Light in Polymer Science: Photochemical Processes to Manipulate Polymer Formation, Structure, and Properties. *Polym. Chem.* **2014**, *5* (7), 2187–2201.
- (5) Ruskowitz, E. R.; DeForest, C. A. Photoresponsive Biomaterials for Targeted Drug Delivery

- 1
2
3 and 4D Cell Culture. *Nat. Rev. Mater.* **2018**, *3*, 17087.
4
5 (6) Kharkar, P. M.; Kiick, K. L.; Kloxin, A. M. Designing Degradable Hydrogels for Orthogonal
6 Control of Cell Microenvironments. *Chem. Soc. Rev.* **2013**, *42* (17), 7335–7372.
7
8 (7) Bochet, C. G. Photolabile Protecting Groups and Linkers. *J. Chem. Soc. Perkin Trans. 1*
9 **2002**, No. 2, 125–142.
10
11 (8) Griffin, D. R.; Borrajo, J.; Soon, A.; Acosta-Vélez, G. F.; Oshita, V.; Darling, N.; Mack, J.;
12 Barker, T.; Iruela-Arispe, M. L.; Segura, T. Hybrid Photopatterned Enzymatic Reaction
13 (HyPER) for in Situ Cell Manipulation. *ChemBioChem* **2014**, *15* (2), 233–242.
14
15 (9) Lee, J.; Hee Ku, K.; Kim, J.; Jun Lee, Y.; Gyu Jang, S.; Kim, B. J. Light-Responsive, Shape-
16 Switchable Block Copolymer Particles. *J. Am. Chem. Soc.* **2019**, *141* (38), 15348–15355.
17
18 (10) Li, Z.; Davidson-Rozenfeld, G.; Vázquezvázquez-González, M.; Fadeev, M.; Zhang, J.;
19 Tian, H.; Willner, I. Multi-Triggered Supramolecular DNA/Bipyridinium Dithienylethene
20 Hydrogels Driven by Light, Redox, and Chemical Stimuli for Shape-Memory and Self-
21 Healing Applications. *J. Am. Chem. Soc.* **2018**, *140* (50), 17691–17701.
22
23 (11) van der Vlies, A. J.; Barua, N.; Nieves-Otero, P. A.; Platt, T. G.; Hansen, R. R. On Demand
24 Release and Retrieval of Bacteria from Microwell Arrays Using Photodegradable Hydrogel
25 Membranes. *ACS Appl. Bio Mater.* **2019**, *2*, 266–276.
26
27 (12) Ramanan, V. V.; Katz, J. S.; Guvendiren, M.; Cohen, E. R.; Marklein, R. A.; Burdick, J. A.
28 Photocleavable Side Groups to Spatially Alter Hydrogel Properties and Cellular
29 Interactions. *J. Mater. Chem.* **2010**, *20* (40), 8920–8926.
30
31 (13) Houck, H. A.; Blasco, E.; Du Prez, F. E.; Barner-Kowollik, C. Light-Stabilized Dynamic
32 Materials. *J. Am. Chem. Soc.* **2019**, *141* (31), 12329–12337.
33
34 (14) Rosales, A. M.; Vega, S. L.; DelRio, F. W.; Burdick, J. A.; Anseth, K. S. Hydrogels with
35 Reversible Mechanics to Probe Dynamic Cell Microenvironments. *Angew. Chemie Int. Ed.*
36 **2017**, *56* (40), 12132–12136.
37
38
39
40
41
42
43
44
45
46
47
48
49
50
51
52
53
54
55
56
57
58
59
60

- 1
2
3 (15) LeValley, P. J.; Tibbitt, M. W.; Noren, B.; Kharkar, P.; Kloxin, A. M.; Anseth, K. S.; Toner,
4 M.; Oakey, J. Immunofunctional Photodegradable Poly(Ethylene Glycol) Hydrogel
5 Surfaces for the Capture and Release of Rare Cells. *Colloids Surfaces B Biointerfaces*
6 **2019**, *174*, 483–492.
7
8
9
10
11 (16) Norris, S. C. P.; Delgado, S. M.; Kasko, A. M. Mechanically Robust Photodegradable
12 Gelatin Hydrogels for 3D Cell Culture and: In Situ Mechanical Modification. *Polym. Chem.*
13 **2019**, *10* (23), 3180–3193.
14
15
16
17 (17) Kohman, R. E.; Cha, S. S.; Man, H. Y.; Han, X. Light-Triggered Release of Bioactive
18 Molecules from DNA Nanostructures. *Nano Lett.* **2016**, *16* (4), 2781–2785.
19
20
21
22 (18) Gawade, P. M.; Shadish, J. A.; Badeau, B. A.; DeForest, C. A. Logic-Based Delivery of
23 Site-Specifically Modified Proteins from Environmentally Responsive Hydrogel
24 Biomaterials. *Adv. Mater.* **2019**, *31* (33), 1902462.
25
26
27
28 (19) Kloxin, A. M.; Kasko, A. M.; Salinas, C. N.; Anseth, K. S. Photodegradable Hydrogels for
29 Dynamic Tuning of Physical and Chemical Properties. *Science (80-.)*. **2009**, *324*, 59–63.
30
31
32
33 (20) Kloxin, A. M.; Tibbitt, M. W.; Kasko, A. M.; Fairbairn, J. A.; Anseth, K. S. Tunable Hydrogels
34 for External Manipulation of Cellular Microenvironments through Controlled
35 Photodegradation. *Adv. Mater.* **2010**, *22* (1), 61–66.
36
37
38
39 (21) Griffin, D. R.; Kasko, A. M. Photodegradable Macromers and Hydrogels for Live Cell
40 Encapsulation and Release. *J. Am. Chem. Soc.* **2012**, *134* (31), 13103–13107.
41
42
43
44 (22) Griffin, D. R.; Kasko, A. M. Photoselective Delivery of Model Therapeutics from Hydrogels.
45 *ACS Macro Lett.* **2012**, *1* (11), 1330–1334.
46
47
48
49 (23) Holmes, C. P. Model Studies for New O-Nitrobenzyl Photolabile Linkers: Substituent
50 Effects on the Rates of Photochemical Cleavage. *J. Org. Chem.* **1997**, *62* (8), 2370–2380.
51
52
53
54 (24) Salerno, C. P.; Cleaves, H. J. A Simple Synthesis of Photolabile A-Methyl Nitrobenzyl
55 Compounds. *Synth. Commun.* **2004**, *34* (13), 2379–2386.
56
57
58
59
60

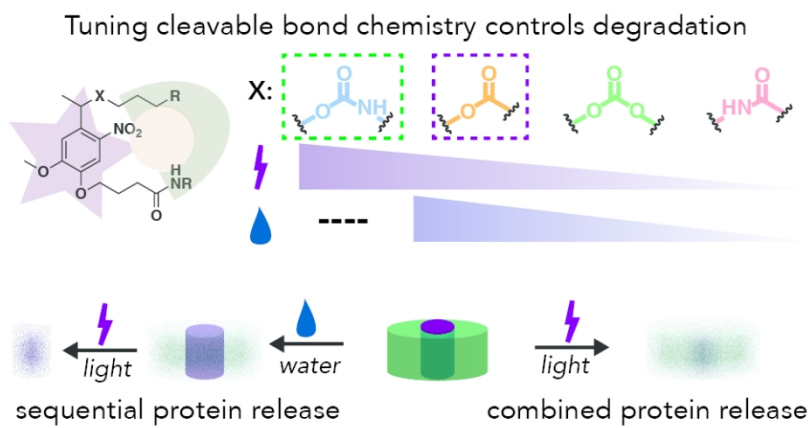
- 1
2
3 (25) Griffin, D. R.; Schlosser, J. L.; Lam, S. F.; Nguyen, T. H.; Maynard, H. D.; Kasko, A. M.
4
5 Synthesis of Photodegradable Macromers for Conjugation and Release of Bioactive
6
7 Molecules. *Biomacromolecules* **2013**, *14* (4), 1199–1207.
8
9
10 (26) Deforest, C. A.; Tirrell, D. A. A Photoreversible Protein-Patterning Approach for Guiding
11
12 Stem Cell Fate in Three-Dimensional Gels. *Nat. Mater.* **2015**, *14*, 523–531.
13
14 (27) Mikkelsen, R. J. T.; Grier, K. E.; Mortensen, K. T.; Nielsen, T. E.; Qvortrup, K. Photolabile
15
16 Linkers for Solid-Phase Synthesis. *ACS Comb. Sci.* **2018**, *20* (7), 377–399.
17
18 (28) DeForest, C. A.; Anseth, K. S. Cytocompatible Click-Based Hydrogels with Dynamically
19
20 Tunable Properties through Orthogonal Photoconjugation and Photocleavage Reactions.
21
22 *Nat. Chem.* **2011**, *3* (12), 925–931.
23
24
25 (29) McKinnon, D. D.; Brown, T. E.; Kyburz, K. A.; Kiyotake, E.; Anseth, K. S. Design and
26
27 Characterization of a Synthetically Accessible, Photodegradable Hydrogel for User-
28
29 Directed Formation of Neural Networks. *Biomacromolecules* **2014**, *15* (7), 2808–2816.
30
31 (30) Kharkar, P. M.; Kiick, K. L.; Kloxin, A. M. Design of Thiol- and Light-Sensitive Degradable
32
33 Hydrogels Using Michael-Type Addition Reactions. *Polym. Chem.* **2015**, *6* (31), 5565–
34
35 5574.
36
37
38 (31) Kharkar, P. M.; Scott, R. A.; Olney, L. P.; LeValley, P. J.; Maverakis, E.; Kiick, K. L.; Kloxin,
39
40 A. M. Controlling the Release of Small, Bioactive Proteins via Dual Mechanisms with
41
42 Therapeutic Potential. *Adv. Healthc. Mater.* **2017**, *6* (24), 1700713.
43
44
45 (32) Claaßen, C.; Claaßen, M. H.; Gohl, F.; Tovar, G. E. M.; Borchers, K.; Southan, A.
46
47 Photoinduced Cleavage and Hydrolysis of O-Nitrobenzyl Linker and Covalent Linker
48
49 Immobilization in Gelatin Methacryloyl Hydrogels. *Macromol. Biosci.* **2018**, *18* (9),
50
51 1800104.
52
53
54 (33) Šolomek, T.; Mercier, S.; Bally, T.; Bochet, C. G. Photolysis of Ortho-Nitrobenzylic
55
56 Derivatives: The Importance of the Leaving Group. *Photochem. Photobiol. Sci.* **2012**, *11*
57
58
59
60

- 1
2
3 (3), 548–555.
4
5 (34) Shi, Y.; Truong, V. X.; Kulkarni, K.; Qu, Y.; Simon, G. P.; Boyd, R. L.; Perlmutter, P.;
6
7 Lithgow, T.; Forsythe, J. S. Light-Triggered Release of Ciprofloxacin from an in Situ
8
9 Forming Click Hydrogel for Antibacterial Wound Dressings. *J. Mater. Chem. B* **2015**, *3* (45),
10
11 8771–8774.
12
13
14 (35) Tibbitt, M. W.; Kloxin, A. M.; Sawicki, L. A.; Anseth, K. S. Mechanical Properties and
15
16 Degradation of Chain and Step-Polymerized Photodegradable Hydrogels. *Macromolecules*
17
18 **2013**, *46* (7), 2785–2792.
19
20
21 (36) Kloxin, A. M.; Kloxin, C. J.; Bowman, C. N.; Anseth, K. S. Mechanical Properties of
22
23 Cellularly Responsive Hydrogels and Their Experimental Determination. *Adv. Mater.* **2010**,
24
25 *22* (31), 3484–3494.
26
27
28 (37) Treloar, L. R. . *The Physics of Rubber Elasticity*, Oxford University Press: Oxford, 1975.
29
30 (38) Zhong, M.; Wang, R.; Kawamoto, K.; Olsen, B. D.; Johnson, J. A. Quantifying the Impact
31
32 of Molecular Defects on Polymer Network Elasticity. *Science (80-.)*. **2016**, *353*, 1264–
33
34 1268.
35
36
37 (39) Aubé, J. A New Twist on Amide Solvolysis. *Angew. Chemie Int. Ed.* **2012**, *51* (13), 3063–
38
39 3065.
40
41 (40) Rinnová, M.; Nováková, M.; Kašička, V.; Jiráček, J. Side Reactions during Photochemical
42
43 Cleavage of an Alpha-Methyl-6-Nitroveratryl-Based Photolabile Linker. *J. Pept. Sci.* **2000**,
44
45 *6* (8), 355–365.
46
47
48 (41) Shen, J.; Burgess, D. J. Accelerated in Vitro Release Testing of Implantable PLGA
49
50 Microsphere/PVA Hydrogel Composite Coatings. *Int. J. Pharm.* **2012**, *422*, 341–348.
51
52 (42) Coutinho, D. F.; Sant, S. V.; Shin, H.; Oliveira, J. T.; Gomes, M. E.; Neves, N. M.;
53
54 Khademhosseini, A.; Reis, R. L. Modified Gellan Gum Hydrogels with Tunable Physical
55
56 and Mechanical Properties. *Biomaterials* **2010**, *31* (29), 7494–7502.
57
58
59
60

- 1
2
3 (43) Browning, M. B.; Cereceres, S. N.; Luong, P. T.; Cosgriff-Hernandez, E. M. Determination
4 of the in Vivo Degradation Mechanism of PEGDA Hydrogels. *J. Biomed. Mater. Res. Part*
5 *A* **2014**, *102A* (12), 4244–4251.
6
7
8
9 (44) Brown, R. S.; Bennet, A. J.; Slebocka-Tilk, H. Recent Perspectives Concerning the
10 Mechanism of H₃O⁺- and Hydroxide-Promoted Amide Hydrolysis. *Acc. Chem. Res.* **1992**,
11 *25* (11), 481–488.
12
13
14
15 (45) Day, J. N. E.; Ingold, C. K. Mechanism and Kinetics of Carboxylic Ester Hydrolysis and
16 Carboxyl Esterification. *Trans. Faraday Soc.* **1941**, *37*, 686–705.
17
18
19 (46) Dittert, L. W.; Higuchi, T. Rates of Hydrolysis of Carbamate and Carbonate Esters in
20 Alkaline Solution. *J. Pharm. Sci.* **1963**, *52* (9), 852–857.
21
22
23
24 (47) Maverakis, E.; L; Cornelius, L. A.; Bowen, G. M.; Phan, T.; Patel, F. B.; Fitzmaurice, S.;
25 He, Y.; Burrall, B.; Duong, C.; Kloxin, A. M.; Sultani, H.; Wilken, R.; Martinez, S. R.; Patel,
26 F. Metastatic Melanoma – A Review of Current and Future Treatment Options. *Acta Derm.*
27 *Venerol.* **2015**, *95* (5), 516–524.
28
29
30
31 (48) Rehmann, M. S.; Skeens, K. M.; Kharkar, P. M.; Ford, E. M.; Maverakis, E.; Lee, K. H.;
32 Kloxin, A. M. Tuning and Predicting Mesh Size and Protein Release from Step Growth
33 Hydrogels. *Biomacromolecules* **2017**, *18* (10), 3131–3142.
34
35
36 (49) Aziz, A. H.; Wahlquist, J.; Sollner, A.; Ferguson, V.; DelRio, F. W.; Bryant, S. J. Mechanical
37 Characterization of Sequentially Layered Photo-Clickable Thiol-Ene Hydrogels. *J. Mech.*
38 *Behav. Biomed. Mater.* **2017**, No. 65, 454–465.
39
40
41 (50) Azagarsamy, M. A.; Marozas, I. A.; Spaans, S.; Anseth, K. S. Photoregulated Hydrazone-
42 Based Hydrogel Formation for Biochemically Patterning 3D Cellular Microenvironments.
43 *ACS Macro Lett.* **2016**, *5* (1), 19–23.
44
45
46 (51) Azagarsamy, M. A.; Anseth, K. S. Wavelength-Controlled Photocleavage for the
47 Orthogonal and Sequential Release of Multiple Proteins. *Angew. Chemie - Int. Ed.* **2013**,
48
49
50
51
52
53
54
55
56
57
58
59
60

1
2
3 52 (51), 13803–13807.
4

- 5 (52) Raman, R.; Hua, T.; Gwynne, D.; Collins, J.; Tamang, S.; Zhou, J.; Esfandiary, T.; Soares,
6 V.; Pajovic, S.; Hayward, A.; Langer, R.; Traverso, G. Light-Degradable Hydrogels as
7 Dynamic Triggers for Gastrointestinal Applications. *Sci. Adv.* **2020**, *6* (3), eaay0065.
8
9
10
11
12
13
14
15
16
17
18
19
20
21
22
23
24
25
26
27
28
29
30
31
32
33
34
35
36
37
38
39
40
41
42
43
44
45
46
47
48
49
50
51
52
53
54
55
56
57
58
59
60



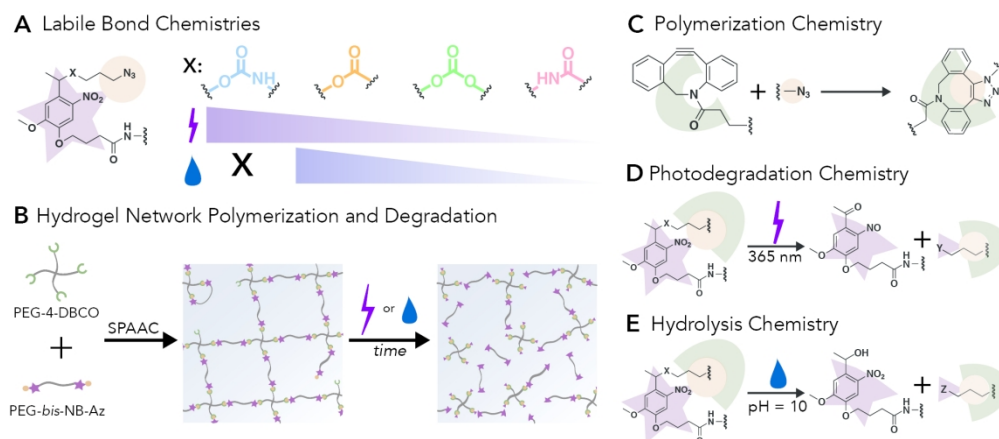


Figure 1. Overview of approach. (A) Nitrobenzyl (NB) moieties were synthesized to have various labile bond chemistries, X: carbamate (blue), ester (orange), carbonate (green), or amide (pink). (B) Hydrogel networks formed with NB containing crosslinks were degraded over short time scales by light irradiation or over long time scales by incubation in aqueous conditions. (C) Hydrogels were polymerized using a SPAAC between PEG-4-DBCO and photodegradable PEG-bis-NB-azide (Az) to form triazole linkages. (D) Upon irradiation with 365 nm light the incorporated NB moiety undergoes an irreversible photocleavage event that breaks hydrogel crosslinks, leading to hydrogel erosion. The cleavable bond, X, dictates the rate of photodegradation and the functionality of the cleavage products formed, Y. (E) Additionally, the nature of the cleavable bond influences the ability of the hydrogel to degrade in aqueous environments; here, a hydroxyl is shown, which would be generated upon hydrolysis of NB-ester, NB-carbonate, and NB-carbamate linkers, whereas an amine would be generated upon hydrolysis of NB-amide linkers. The functionality of the hydrolysis cleavage product is represented by, Z.

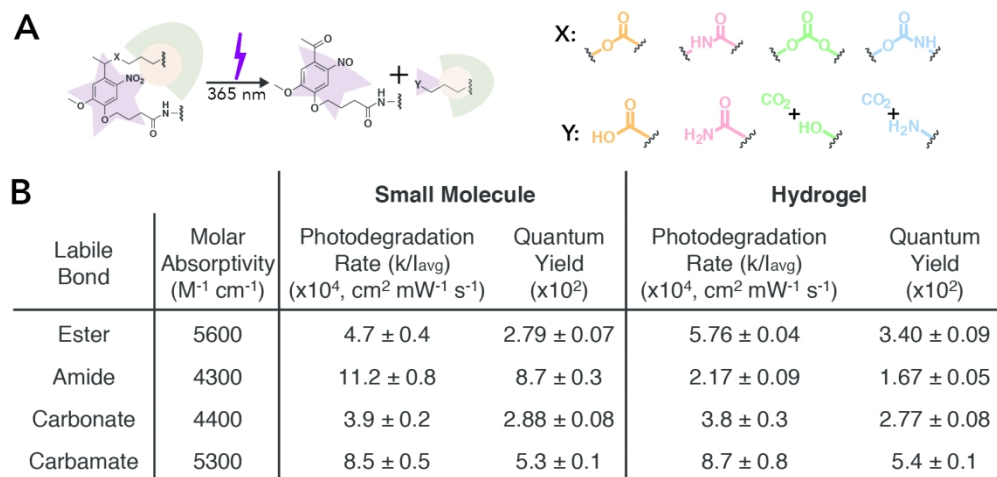


Figure 2. Rate of small molecule and hydrogel degradation in response to light. (A) The NB moiety incorporated within the hydrogel backbone undergoes a β -elimination reaction upon 365 nm light irradiation. Four different photocleavable bonds, X, were investigated, all of which lead to different cleavage products, Y (as confirmed by NMR and mass spectrometry, Figures S21 – S24 and Tables S1 – S4). (B) Small molecule NBs ($I_0 = 10 \text{ mW cm}^{-2}$ resulting in an $I_{\text{avg}} = 7.8 \text{ mW cm}^{-2}$) and photolabile hydrogels ($I_0 = 4 \text{ mW cm}^{-2}$ resulting in an $I_{\text{avg}} = 3.9 \text{ mW cm}^{-2}$) were irradiated with 365 nm light to determine the first order photodegradation rate and quantum yield. The molar absorptivity was determined using the absorbance of each small molecule NB moiety at 365 nm. First order rate constants were determined for each of the four NB groups with different cleavable bonds in solution and within hydrogels (Figure S20 and S27) and used to calculate the quantum yield. All formulations (NB-ester vs. NB-Amide vs. NB-carbonate vs. NB-carbamate) were found to be statistically different except that determined for the ester and carbonate in solution and for the amide and carbonate in hydrogels ($p = 0.05$). For full statistical analysis see Tables S6 – S8. The data shown illustrate the mean ($n = 3$) with error representing standard error.

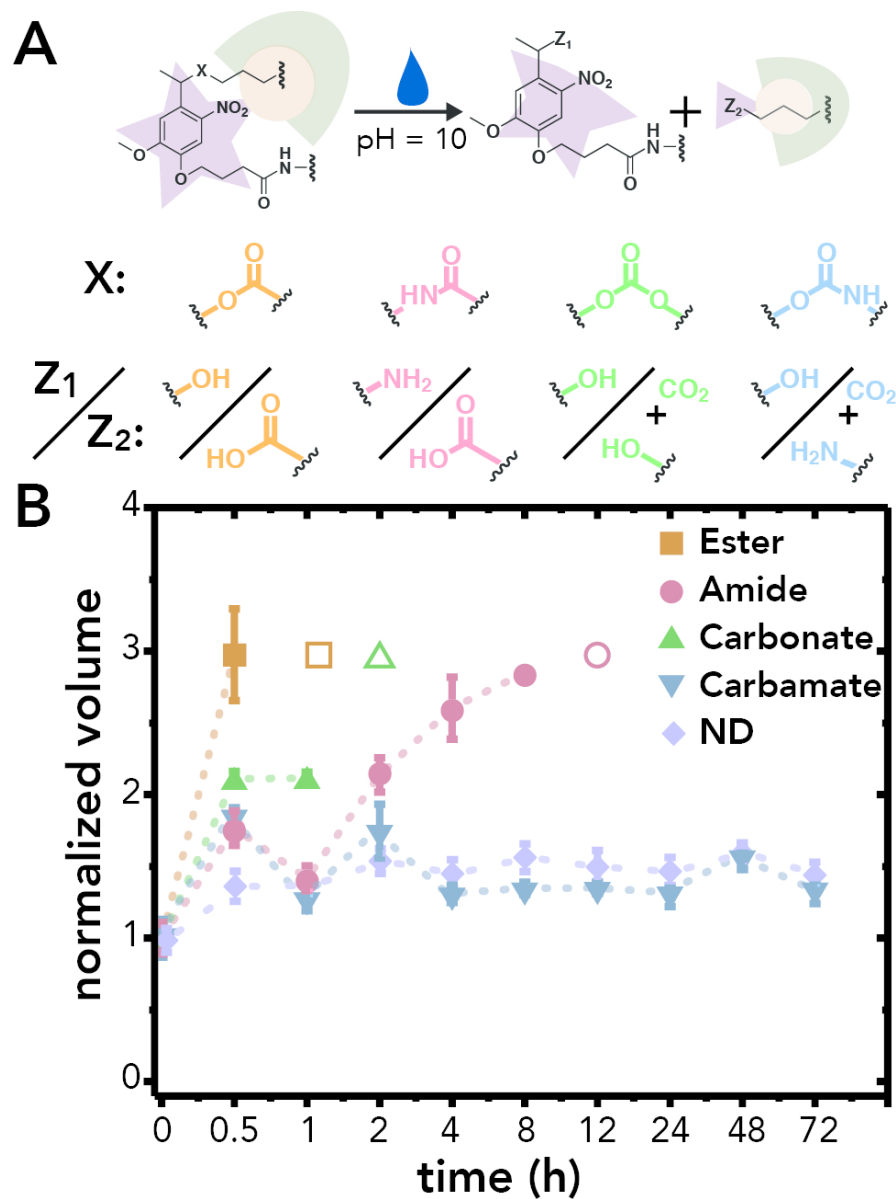
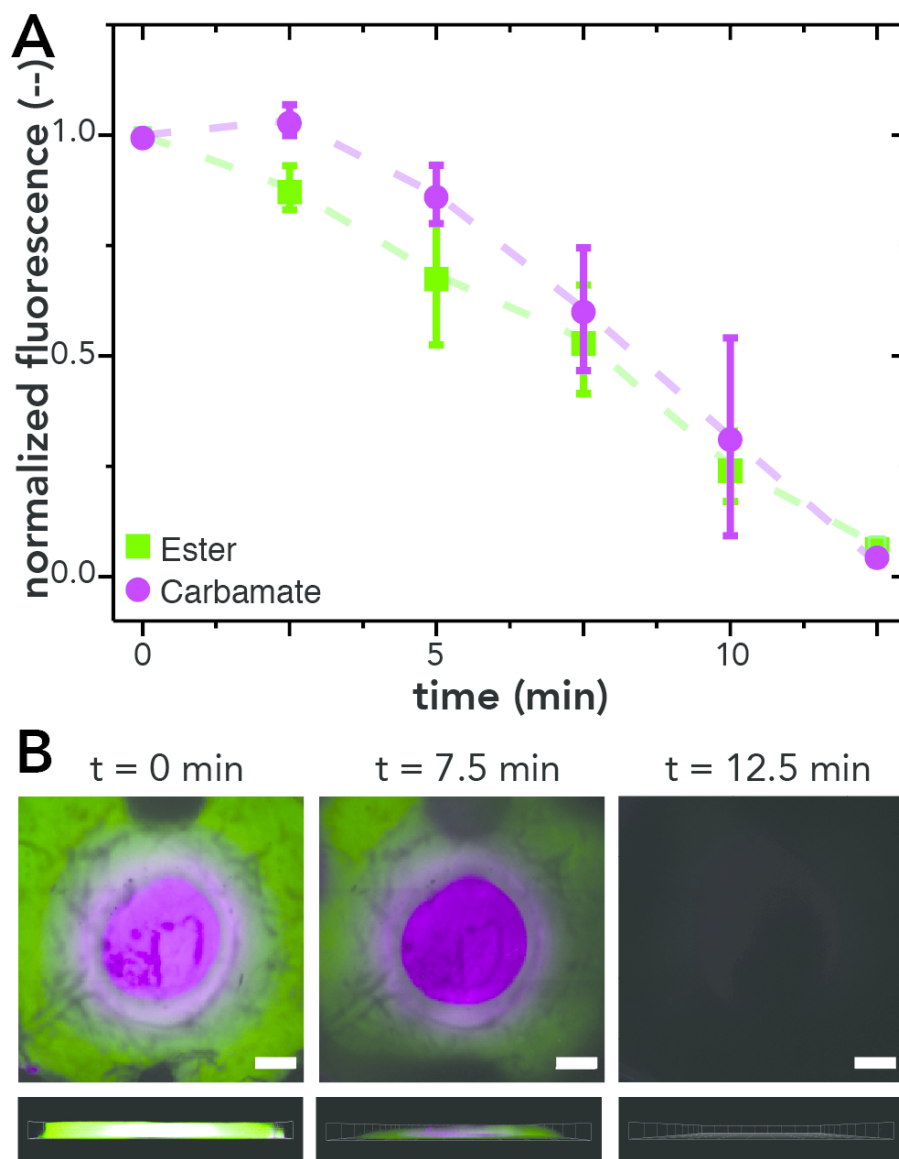


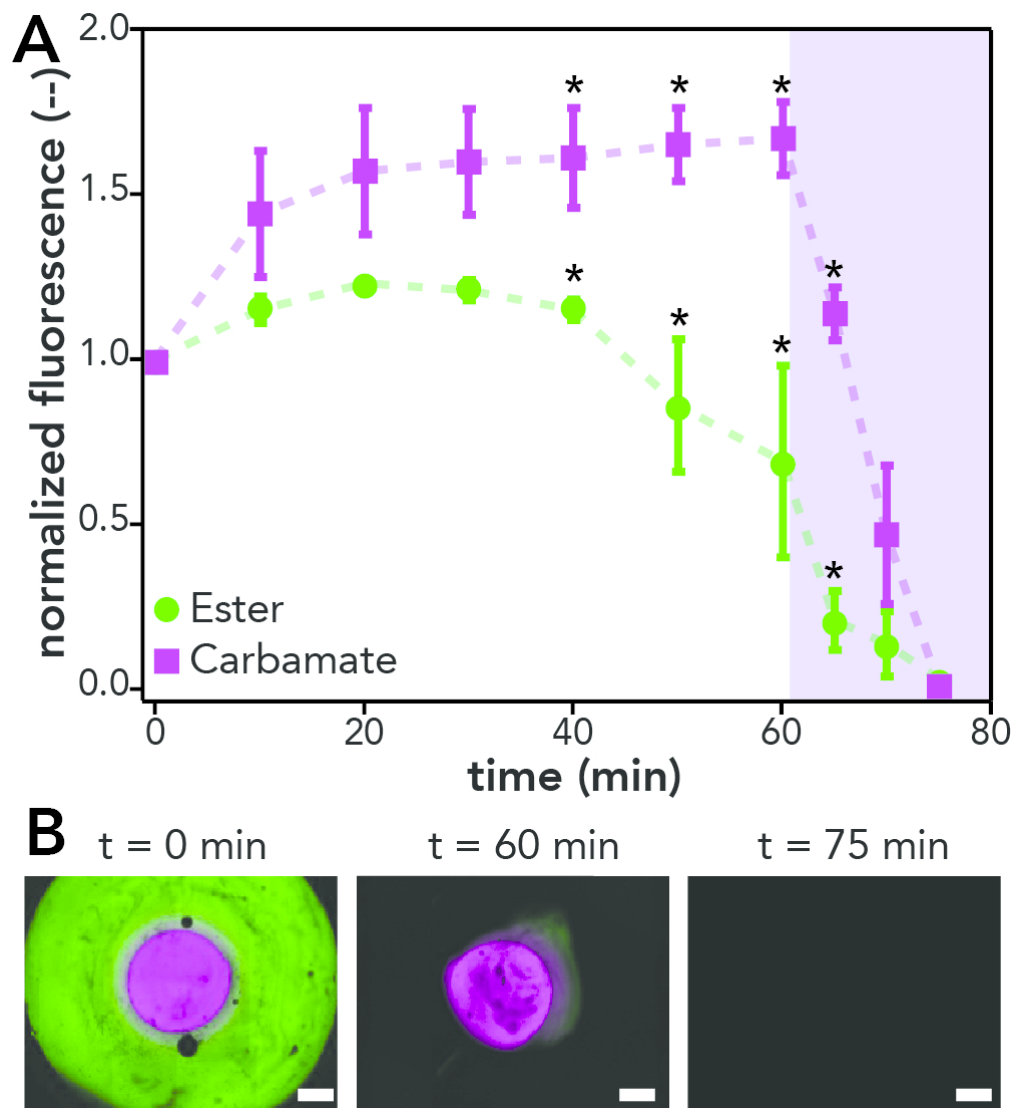
Figure 3. Hydrolysis of NB-linked hydrogels. (A) The cleavable bond (X) of the NB group dictates the rate of hydrogel hydrolysis and the products formed, where Z1 and Z2 represent the products formed on the NB ring and cleaved chain, respectively. (B) Hydrogel volume was monitored over 72 h as a semi-quantitative measure of the rate of hydrolysis, where hydrogels were incubated in PBS pH = 10 for accelerated hydrolysis. Hydrogels crosslinked with ether-linked PEG-bis-azide served as a non-degradable (ND) control. The empty shapes indicate complete hydrogel degradation which occurred at < 1 h for NB-ester, < 2 h for NB-carbonate, and < 12 h for NB-amide. The volume was normalized to the equilibrium swollen hydrogel volume at $t = 0$ h. The data shown illustrate the mean ($n = 3$) with error bars representing standard error.

81x110mm (300 x 300 DPI)



45 Figure 4. Combinatorial protein release from dually functional concentric cylinder hydrogels. NB-ester (BSA-
46 AF488 labeled) and NB-carbamate (BSA-AF647 labeled) dually functional concentric cylinder hydrogels were
47 formed and subsequently irradiated with light (365 nm, $I_0 = 10 \text{ mW cm}^{-2}$) to demonstrate quantitatively
48 the combined release of multiple components dictated by photodegradation kinetics of the respective
49 linkers. (A) The normalized intensity of each region of the concentric cylinder hydrogels was monitored over
50 time and observed to decrease at a similar rate for both layers. (B) Representative images of the surface
51 (top) and side (bottom, 200 μm z-stack) of concentric cylinder hydrogels at 0 min (left), 7.5 min (middle),
52 and 12.5 min (right). The data shown illustrate the mean ($n = 3$) with error bars representing standard
53 error. No statistical differences observed between compositions at each time point ($p = 0.05$). Scale bars
54 500 μm .

83x110mm (300 x 300 DPI)



42 Figure 5. Sequential protein release from dually functional concentric cylinder hydrogels. NB-ester (BSA-
43 AF488 labeled) and NB-carbamate (BSA-AF647 labeled) concentric cylinder hydrogels were formed and
44 subsequently incubated under accelerated hydrolysis conditions (PBS pH = 10) for 60 min followed by
45 irradiation with light (365 nm, $I_0 = 10 \text{ mW cm}^{-2}$). (A) The ester hydrogel layer (green) was observed to
46 degrade during incubation in basic conditions, whereas the carbamate layer (purple) was not observed to
47 degrade until light irradiation. (B) Representative images of the hydrogel at 0 min (left), 60 min (middle),
48 and 75 min (right). The data shown illustrate the mean ($n = 3$) with error bars representing standard error
49 ($p = 0.05$). Scale bars 500 μm .

50 84x93mm (300 x 300 DPI)

